SUDDEN JUMPS IN TIME-MEAN VALUES OF LIFT COEFFICIENT FOR A CIRCULAR CYLINDER IN ORBITAL MOTION IN A UNIFORM FLOW

L. Baranyi

University of Miskolc, Miskolc, Hungary

ABSTRACT

A finite difference solution is presented for 2-D laminar unsteady flow around a circular cylinder in orbital motion placed in a uniform flow in the Reynolds number domain of Re=100-180. Abrupt jumps were found in the time-mean values of the lift coefficient under lock-in conditions. The phenomenon was investigated by computations at different values of Re and amplitude of in-line oscillation and at different angles of attack. Plotting against ellipticity revealed two states of vortex shedding.

1. INTRODUCTION

Flow-induced vibration of structures is encountered in various fields of engineering such as civil engineering, power generation and transmission, ocean engineering and offshore industry, the aerospace industry, and wind engineering. Bridges, tall buildings, or smoke stacks may undergo oscillations in a strong wind; closely packed tubes in heat exchangers move in oval orbits at high flow velocities; suspended spans of pipelines vibrate in strong currents and/or waves, and so on.

These motions are often not limited to one direction, i.e. they oscillate in both transverse and in-line directions. Oscillation in two directions can result in an orbital motion of the body, in which case it follows an elliptical path.

Oscillatory flow has been fairly widely researched (e.g. Bearman et al (1985), Sarpkaya (1986)), as have oscillating cylinders in uniform flow (e.g. Mahfouz and Badr (2000); Baranyi (2003a)). Also, in fluid at rest, an orbiting cylinder has been investigated numerically by Teschauer et al (2002), while Stansby and Rainey (2001) investigated a cylinder which was orbiting and rotating. However, research on an orbiting cylinder in uniform flow seems to have been ignored.

Earlier the author carried out computational investigations on a cylinder in orbital motion in a uniform stream at three Reynolds numbers, *Re*=130, 160 and 180 (Baranyi 2003b)). The orbital path resulted from the superposition of in-line and transverse oscillations, with frequencies of 85% that of the vortex shedding frequency from a stationary

cylinder at that Reynolds number. The non-dimensional amplitude of oscillation in the in-line direction A_x was kept constant, while that of the transverse oscillation A_y was varied. At some A_y values sudden jumps were observed under lock-in conditions in the time-mean value of the lift coefficient $\overline{C}_L$ and in the root-mean-square (*rms*) values of lift and drag coefficients.

These unexpected results led the author to further investigate this phenomenon. Computations were repeated at several other *Re* and A_x values and results were plotted against ellipticity. It appears as if there are two states of vortex shedding. Computational results for a finer mesh gave practically the same jumps on the curves.

To remove the symmetry of the geometry and flow conditions the direction of the free stream velocity *U* was changed by introducing an attack angle. Results obtained for some values agreed quite well with those of to the original arrangement.

This paper introduces results from the attempts made so far to clarify the phenomenon of the sudden jumps.

2. GOVERNING EQUATIONS AND NUMERICAL METHOD

The dimensionless governing equations are the two components of the Navier-Stokes equations, the continuity equation and the pressure Poisson equation written in a non-inertial system fixed to the orbiting cylinder. The Navier-Stokes equations can be written as

$$\frac{\partial u}{\partial t} + u\frac{\partial u}{\partial x} + v\frac{\partial u}{\partial y} = -\frac{\partial p}{\partial x} + \frac{1}{Re}\nabla^2 u - a_{0x}, \quad (1)$$

$$\frac{\partial v}{\partial t} + u\frac{\partial v}{\partial x} + v\frac{\partial v}{\partial y} = -\frac{\partial p}{\partial y} + \frac{1}{Re}\nabla^2 v - a_{0y}. \quad (2)$$

In the equations above ∇^2 is the two-dimensional (2-D) Laplacian operator, *x*, *y* are Cartesian co-ordinates, *u*, *v* are the *x*, *y* components of velocity in the system fixed to the cylinder and a_{0x}, a_{0y} are the

components of cylinder acceleration. Here Re is the Reynolds number defined as $Re = Ud/\nu$ where d is the diameter of the cylinder, U is the upstream velocity and ν is the kinematic viscosity. In these equations the body force is included in the pressure terms. The equation of continuity has the form

$$D = \frac{\partial u}{\partial x} + \frac{\partial v}{\partial y} = 0 \qquad (3)$$

where D is the dilation.

Although theoretically equations (1)-(3) are applicable for the determination of the three unknowns u, v and p, according to Harlow and Welch (1965) it is advisable to use a separate equation for pressure p. Taking the divergence of the Navier-Stokes equations yields the Poisson equation for pressure

$$\nabla^2 p = 2\left[\frac{\partial u}{\partial x}\frac{\partial v}{\partial y} - \frac{\partial u}{\partial y}\frac{\partial v}{\partial x}\right] - \frac{\partial D}{\partial t}. \qquad (4)$$

Although in this equation the dilation $D = 0$ by continuity (3), it is advisable to retain its partial derivative with respect to time to reduce numerical errors and to avoid instability. Equations (1), (2) and (4) will be solved while the continuity equation (3) is satisfied at every time step.

No-slip boundary condition is used on the cylinder surface for the velocity and a Neumann-type condition is used for pressure p. A potential flow distribution is assumed far from the cylinder.

Boundary conditions can only be imposed accurately when using boundary fitted co-ordinates. In this way interpolation, often leading to poor solutions, can be omitted. Using unique, single-valued functions, the physical domain bounded by two concentric circles with cylinder radius R_1 and radius of the far field R_2, can be mapped into a rectangular computational domain where the spacing is equidistant in both directions. In the physical domain logarithmically spaced radial cells are used, providing a fine grid scale near the cylinder wall and a coarse grid in the far field.

Using the mapping functions, not specified here, the governing equations and boundary conditions can also be transformed into the computational plane. The transformed equations are solved by using the finite difference method. For further details see e.g. Baranyi and Shirakashi (1999) and Baranyi (2003a).

Figure 1 shows the flow arrangement. The motion of the centre of the cylinder with unit diameter is specified as follows:

$$x_0(t) = A_x \cos(2\pi f_x t); \quad y_0(t) = A_y \sin(2\pi f_x t) \qquad (5)$$

where A_x, A_y and f_x, f_y are the dimensionless amplitudes and frequencies of oscillations in x and y directions, respectively. In Figure 1 U is the free stream velocity. Here $f_x = f_y$ which for nonzero A_x, A_y amplitudes gives an ellipse, shown in the dotted line in Figure 1. The orbital path will become a circle when the two amplitudes are equal to each other. If one of the amplitudes is zero, in-line or transverse oscillation is obtained. When both amplitudes are zero the cylinder becomes stationary.
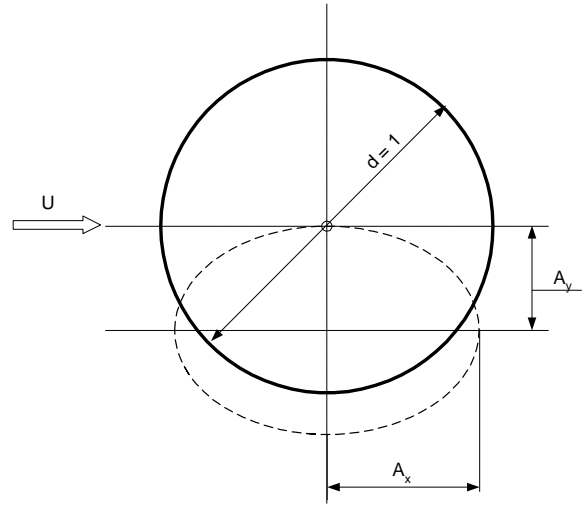

Figure 1 : Cylinder in orbital motion

3. COMPUTATIONAL RESULTS

Computational results for flow around a cylinder in orbital motion were shown for four cases in an earlier paper of the author (Baranyi, 2003b).

The dimensionless frequencies f_x and f_y were kept constant at 85% of the frequency of vortex shedding from a stationary cylinder at that Reynolds number. This value was chosen because lock-in (synchronisation of frequencies for vortex shedding and cylinder oscillation) was desired without very large amplitudes of A_x and A_y. Basically this applies to any further cases shown in this paper.

Reynolds numbers and the dimensionless amplitude of oscillation in the in-line direction A_x were kept fixed and the dimensionless amplitude of oscillation in transverse direction A_y was varied.

Lock-in was observed at all A_y values. One, two or three sudden jumps can be observed in the time-mean values of the lift coefficient $\overline{C}_L$ for the four cases investigated. The shape of the time-history of lift coefficient curves changes abruptly while going

through the critical values of A_y where the jumps take place. It is interesting to note, however, that at the same time the dimensionless vortex shedding frequency, Strouhal number, does not change while passing through the critical A_y value. The slope of curve $\overline{C}_L$ is roughly identical before and after the jump(s).

A typical example is shown in Figure 2, where two sudden jumps can be seen in the curve of $\overline{C}_L$ as a function of dimensionless amplitude of transverse cylinder oscillation A_y. It was found that the shape of the time-history curve of the lift coefficients belonging to A_y values before and after the jump was very different but the frequency of the signal did not change. This change in shape leading to the jumps in $\overline{C}_L$ may be due to a change in the vortex structure.
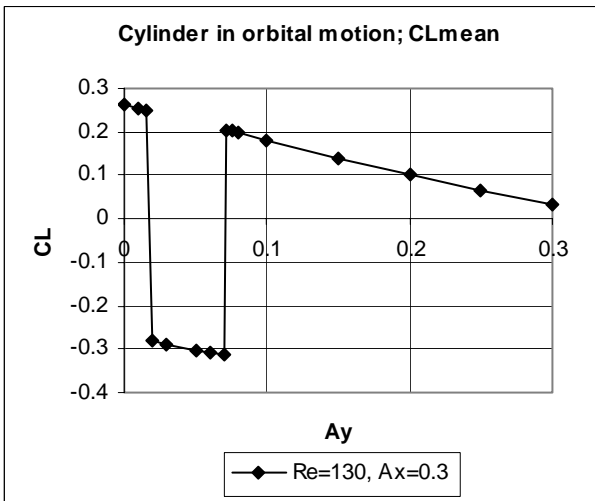

Figure 2 : Time-mean values of lift coefficients vs A_y for Re=130 and A_x=0.3

For all cases analysed previously the time-mean value of the drag coefficient $\overline{C}_D$ seems to be almost completely unaffected by the phenomenon that causes the jumps in $\overline{C}_L$. The root-mean-square (*rms*) values of the lift and drag coefficients were also investigated but are not shown here due to lack of space. The jumps on these curves were less discernable than those on the $\overline{C}_L$ curves. Then computations were extended for cases when $A_y > A_x$ and the time-mean lift curves were re-plotted against ellipticity *E,* defined as

$$E = A_y / A_x$$

(see Figure 3). During that study the maximum

value of ellipticity was 1.2, Reynolds number varied between 130 and 180 and the A_x values were almost unvaried. The locations where the jumps occur are different on every curve. Still, this simple re-scaling reveals that the cases might be classified according to two different states: one with greater lift (generally positive), the other with smaller lift (always negative in the cases studied). Both show an approximately linear decrease with increasing ellipticity *E*, and the difference between the $\overline{C}_L$ values belonging to the two states is approximately constant. Time-mean and *rms* values of other variables (drag and base pressure coefficients) were also re-plotted. Here just the variation of $\overline{C}_D$ versus *E* is shown for the previously investigated four cases (see Figure 4). As can be seen, there are only very small jumps (if any) in the four curves at some critical ellipticity values. For the cases shown it seems that $\overline{C}_D$ is almost completely unaffected by the phenomenon which causes the jumps in $\overline{C}_L$. It can also be seen that $\overline{C}_D$ increases with *Re*.
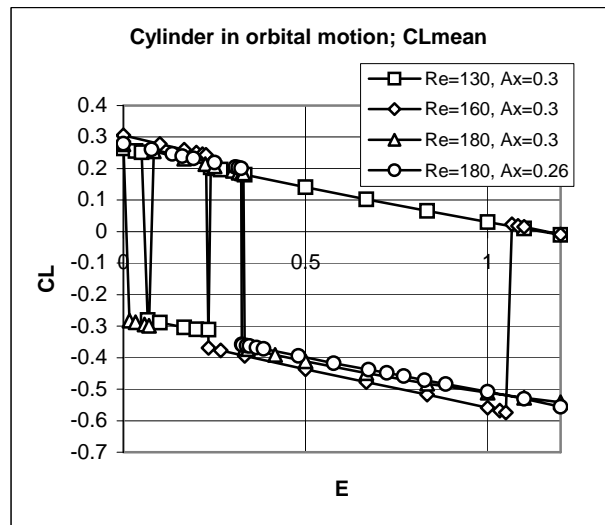

Figure 3 : Time-mean values of lift coefficients vs ellipticity E

For this paper, further computations were made for different A_x and *Re* values to check whether this phenomenon occurs at lower Reynolds numbers as well. The combination of A_x=0.35 and *Re*=100, 110 and 120 assured lock-in condition even when A_y=0 (in-line oscillation). Computed $\overline{C}_L$ values are plotted versus *E* in Figure 5.
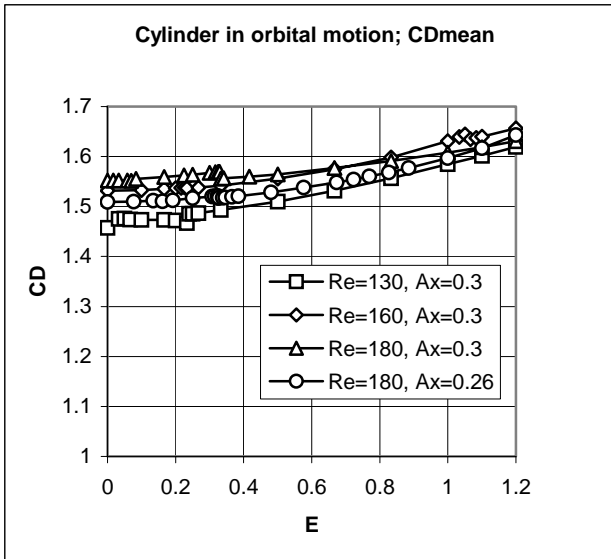
Figure 4 : Time-mean values of drag coefficients vs ellipticity E

It can be seen in Figure 5 that there is no jump for $Re=100$. Computations were carried out for even lower Re numbers and no jumps were found. However, there are jumps for $Re=110$ or 120, so it seems that the critical Reynolds number where the jumps occur in this ellipticity domain belonging to $A_x=0.35$ is around $Re=100$. Curves look similar to those in Figure 3. $\overline{C}_D$ curves for these three cases
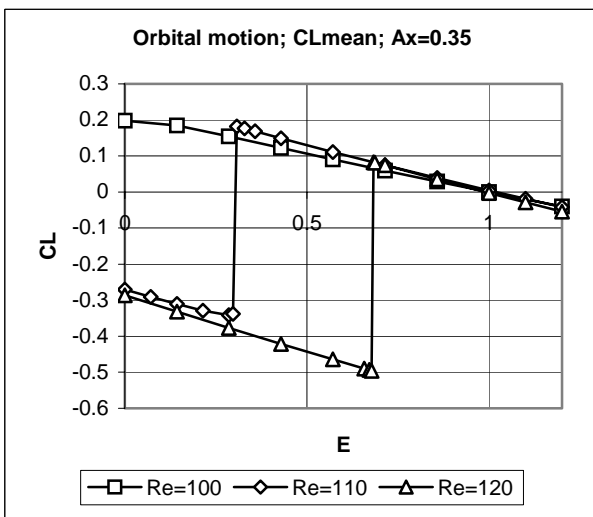

Figure 5 : Time-mean values of lift coefficients vs ellipticity for $A_x=0.35$

are similar to those in Figure 4.

Since Figures 3 and 5 are for A_x values relatively close to each other all seven cases are shown together in one diagram (see Figure 6). The empty signals show cases that have already been investigated (Baranyi, 2003b), and the curves with

filled signals correspond to the curves in Figure 5. In one out of the seven cases there is no jump in $\overline{C}_L$. This is when $Re=100$ and $A_x=0.35$. In every other case there are one or more jumps in $\overline{C}_L$. It can be seen that the two states for the different cases remain in relatively narrow bands.
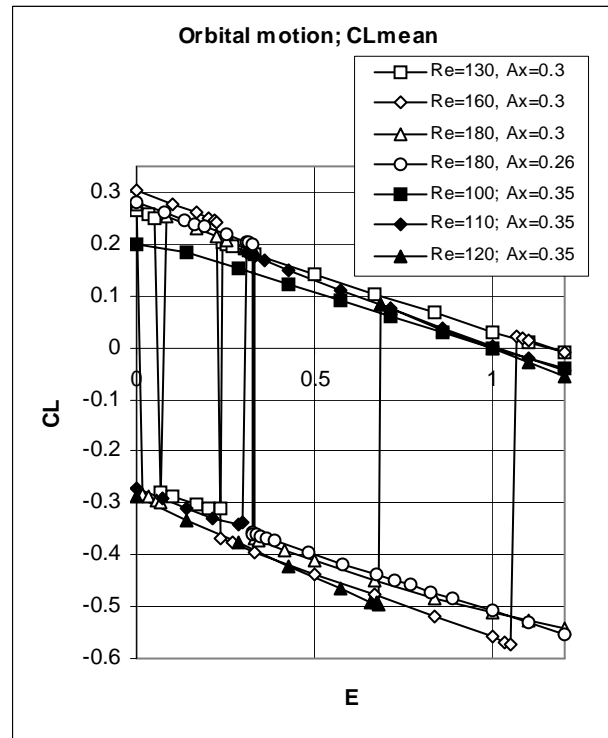

Figure 6 : Time-mean values of lift coefficients vs ellipticity E

The next step was to carry out computations for higher A_x values. Figure 7 shows the variation of $\overline{C}_L$ with ellipticity E for $A_x=0.6$ for three different Reynolds numbers. As can be seen in the figure there are basically two states again for all three cases. These two states are almost the same for the cases of $Re=120$ and 130 and those for $Re=140$ are somewhat shifted. The slopes of the upper curves are roughly identical and their absolute value is greater than for cases at smaller A_x (see Figure 6). Curves belonging to the lower state show less regularity at this A_x value. Curves for $\overline{C}_D$ versus E for $A_x=0.6$, though not shown here, show a similar trend to those shown in Figure 4.

Computations were repeated on a finer mesh for some of the cases shown in this paper. The outcome was that the curves representing the two states did not change at all but there were very small shifts in terms of the locations of jumps in $\overline{C}_L$ versus E.
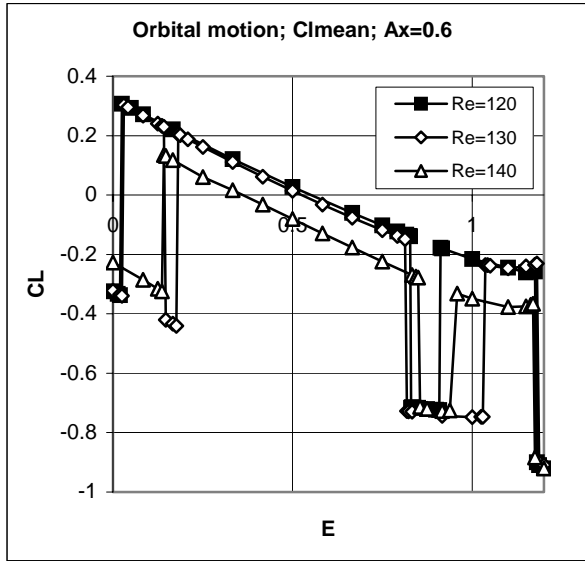
Figure 7 : Time-mean values of lift coefficients vs ellipticity E

The effect of breaking the symmetry of the flow problem was also investigated in order to gather further evidence that these jumps are not due to numerical instabilities. To remove the symmetry in the geometry and boundary conditions the direction of the free stream velocity U was changed. An attack angle α was introduced which is the angle included between velocity U and the x-axis. The case of $\alpha = 0$ can be seen in Figure 1. Computations were carried out for different values of attack angle. The five curves for $\alpha = 0$, ± 0.01, ± 0.1 degrees practically coincide; they appear as one curve when plotted. Computations were then carried out for $\alpha = \pm 1$ deg. Figure 8 shows $\alpha = 0$, ± 0.1, ± 1 deg. As can be seen curves belonging to $\alpha = 0$ and ± 0.1 deg practically coincide, so that it looks as if there were only three curves in the figure. It can be seen that curves belonging to $\alpha = \pm 1$ deg are different from each other and from $\alpha = 0$, but they are very similar to each other in terms of the existence, locations and magnitudes of jumps.

One possible explanation for the jumps is that they may be related to three-dimensional instability, called Mode A instability, occurring at about Re=188 for a stationary cylinder. This instability was proven theoretically by Barkley and Henderson (1996) and Posdziech and Grundmann (2001), and experimentally by Williamson (1996), although Norberg's (2001) experimental results showed a somewhat lower value. However, here it was found that these jumps occurred at lower Reynolds numbers (even at Re=110 and 120) as well, so the 3-D instability explanation seems unlikely, unless instability zones are very different for oscillating cylinders compared to stationary cylinders.

Experimental evidence as in Bearman and Obasaju (1982) and Koide et al (2002) for oscillating cylinders shows that lock-in increases the span-wise correlation of signals and the two-dimensionality of the flow compared to flow around stationary cylinders. Poncet (2002) shows how the 3-D wake behind a circular cylinder can be made 2-D by using lock-in triggered by rotary oscillation of the cylinder. These studies suggest that the jumps are probably not caused by 3-D instabilities. The fact that jumps occurred with different attack angles also supports this view, and further strengthens the author's belief that these jumps are not a consequence of numerical instability either.

The only other explanation that can be offered at this time is that the structure of vortices changes whilst going through the critical ellipticity values, which is represented by the change in the time history of lift coefficient signals as shown in Baranyi (2003b). There is a possibility that bifurcation occurs at these critical values. This phenomenon needs further investigation, perhaps through stability analysis.
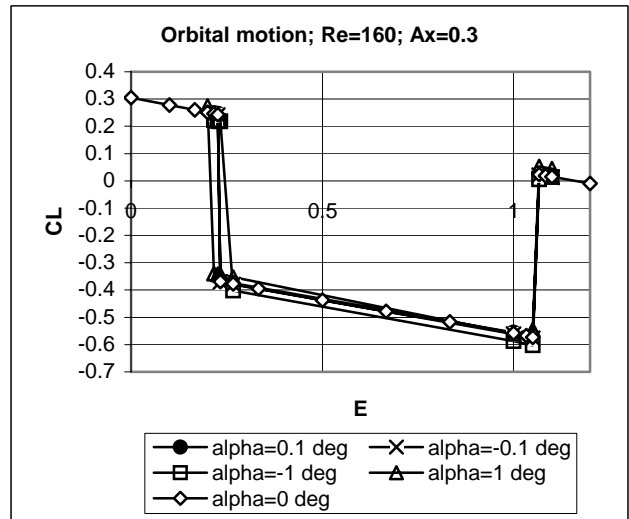

Figure 8 : Time-mean values of lift coefficients vs ellipticity for different angles of attack

4. CONCLUSION

Previous research revealed a rather puzzling phenomenon in which sudden jumps were found when the time-mean values of the lift coefficients $\overline{C}_L$ were plotted against A_y for a cylinder in orbital motion in a uniform flow, while Re and A_x were kept constant. This phenomenon was observed only under lock-in conditions. The main findings of this study were:

- When plotted against ellipticity, it appears that

classification is possible according to two different states: one with greater lift, the other with smaller lift.

- Both states show an approximately linear decrease with increasing ellipticity, and the difference between the $\overline{C}_L$ values belonging to the two states is approximately constant. It seems that the absolute value of the slopes of $\overline{C}_L$ curves increases with increasing A_x. The slopes of the curves are roughly identical, especially on the upper curves, and the absolute value of their slopes is greater than for smaller A_x values. Curves belonging to the lower state show less regularity at A_x=0.6 value.

- At A_x=0.35, *Re* of 100 and below showed no jumps, indicating that there is a limit below which these jumps do not occur.
- The effect of attack angle was investigated, and it was found that attack angle slightly affected curves, but even for $\alpha = \pm 1$ degrees the curves were very similar to each other in terms of locations and magnitudes of jumps.

Further research is needed into the possibility of bifurcation as an explanation for the phenomenon.

5. ACKNOWLEDGEMENTS

6. REFERENCES

Baranyi, L., Shirakashi, M., 1999, Numerical solution for laminar unsteady flow about fixed and oscillating cylinders. *Computer Assisted Mechanics and Engineering Sciences* **6**:263-277.

Baranyi, L., 2003a, Computation of unsteady momentum and heat transfer from a fixed circular cylinder in laminar flow. *Journal of Computational and Applied Mechanics* **4**:13-25.

Baranyi, L., 2003b, Numerical simulation of flow past a cylinder in orbital motion. In *Proceedings of the Conference on Modelling Fluid Flow*, 365-372. Budapest

Barkley, D, Henderson, R. D., 1996, Three-dimensional Floquet stability analysis of the wake of a circular cylinder. *Journal of Fluid Mechanics* **322**:215-241.

Bearman, P.W. Obasaju, E.D., 1982, An experimental study of pressure fluctuations on fixed and oscillating square-section cylinders. *Journal of Fluid Mechanics* **119**:297-321.

Bearman, P. W., Downie, M.J., Graham, J. M. R., Obasaju, E. D., 1985, Forces on cylinders in viscous oscillatory flow at low Keulegan-Carpenter numbers, *Journal of Fluid Mechanics* **154**:337-356.

Harlow, F.H., Welch, J.E., 1965, Numerical calculation of time-dependent viscous incompressible flow of fluid with free surface. *Physics of Fluids* **8**:2182-2189.

Koide, M., Tomida, S., Takahashi, T., Baranyi, L., Shirakashi, M., 2002, Influence of cross-sectional configuration on the synchronization of Kármán vortex shedding with the cylinder oscillation. *JSME International Journal*, Series B **45**(2):249-258.

Mahfouz, F.M., Badr, H.M., 2000, Flow structure in the wake of a rotationally oscillating cylinder. *Journal of Fluids Engineering* **122**:290-301.

Norberg, C., 2001, Flow around a circular cylinder: aspect of fluctuating lift. *Journal of Fluids and Structures* **15**:459-469.

Poncet, P., 2002, Vanishing of B mode in the wake behind a rotationally oscillating cylinder. *Physics of Fluids* **14**(6):2021-2023.

Posdziech, O., Grundmann, R., 2001, Numerical simulation of the flow around an infinitely long circular cylinder in the transition regime. *Theoretical and Computational Fluid Dynamics* **15**:121-141.

Sarpkaya, T., 1986, Force on a circular cylinder in viscous oscillatory flow at low Keulegan-Carpenter numbers. *Journal of Fluid Mechanics* **165**:61-71.

Stansby, P.K., Rainey, R.C.T., 2001, On the orbital response of a rotating cylinder in a current. *Journal of Fluid Mechanics* **439**:87-108.

Teschauer, I., Schäfer, M., Kempf, A., 2002, Numerical simulation of flow induced by a cylinder orbiting in a large vessel. *Journal of Fluids and Structures* **16**(4):435-451.

Williamson, C. H. K., 1996, Vortex dynamics in the cylinder wake. *Annual Review of Fluid Mechanics* **28**:477-539.